Case Report

CT and MRI findings of intracranial extraskeletal mesenchymal chondrosarcoma—a case report and literature review

Jixiang Chu, Huan Ma, Yao Wang, Kun Li, Chengde Liao, Yingying Ding

Department of Radiology, The Third Affiliated Hospital of Kunming Medical University, Yunnan Cancer Hospital, Kunming, China

Correspondence to: Huan Ma, MD, PhD. Department of Radiology, The Third Affiliated Hospital of Kunming Medical University, Yunnan Cancer Hospital, KunZhou Rd. 519, Kunming 650118, China. Email: mahuan347@126.com.

Background: Intracranial extraskeletal mesenchymal chondrosarcoma (EMCS) is a rare neoplasm and often misdiagnosed before histopathological examination due to its rarity. There were few reports previously on the radiological features of intracranial EMCS. We described a 20-year-old male patient with intracranial EMCS focusing on the imaging characteristics.

Case Description: The patient was admitted to our hospital due to headache and dizziness for two months, without nausea, vomiting, limb convulsions and loss of consciousness during the illness. Pre-contrast computed tomography (CT) revealed a large slightly hyperdense mass with irregularly lobulated margins in the right parietal and occipital region and multiple patchy calcifications in peripheral of the lesion. The inner table of right parietal bone adjacent to the mass was compressed, thickened, and eroded. Magnetic resonance imaging (MRI) exhibited intermediate and hypo-intensity on T1-weighted images (T_1WI) and slight hyper-intensity on T2-weighted images (T_2WI) with extremely high intensity rim of cerebral spinal fluid (CSF) and low intensity flow-void vessel. The mass demonstrated heterogeneous remarkable enhancement and "dural tail" sign also was noted. The important imaging signs of this case are irregular calcifications of soft tissue on CT and "dural tail" sign on MRI. The patient underwent tumor resection and was followed up postoperatively with serial MRI every three months. He was alive without obvious clinical symptoms and evidence of recurrence for 9 months. EMCS is a highly invasive tumor and it is difficult to differentiate EMCS from the other intracranial malignant tumors only by clinical characteristics or findings of CT and conventional MR imaging. Radiotherapy and chemotherapy after radical resection are the best treatment choice. Therefore, postoperative patients should be reviewed routinely.

Conclusions: A knowledge of the imaging features could facilitate differentiation of intracranial EMCS, but the final diagnosis depends on pathological examinations. This paper focuses on the imaging characteristics of EMCS and fully describes the details of lesions in order to provide clinicians with effective differential diagnosis information and improve clinical decision-making.

Keywords: Extraskeletal mesenchymal chondrosarcoma (EMCS); computed tomography (CT); magnetic resonance imaging (MRI); case report

Submitted Nov 14, 2021. Accepted for publication Jun 07, 2022.
doi: 10.21037/tcr-21-2547
View this article at: https://dx.doi.org/10.21037/tcr-21-2547

Introduction

Intracranial extraskeletal mesenchymal chondrosarcoma (EMCS) is a rare high-malignant neoplasm with variable prognosis, which only accounts for less than 0.15% of all primary intracranial tumors (1). Due to its rarity, it may not be considered as a differential diagnosis radiologically and it is difficult to make a definite diagnosis before histopathological examination. To our knowledge, previous literatures on intracranial EMCS were mainly about the clinical and pathological manifestations, treatment, and

prognosis (1-3), but the radiological features are few discussed. In this paper, we present a rare case of intracranial EMCS originating from the meninges of the right parietal and occipital regions. The difficulty of CT and MRI diagnosis of intracranial EMCS lies in that the location of tumor onset is not characteristic, and the density and signal are similar to most intracranial tumors. Although the tumor is large, the edema and necrosis are not obvious, and the surrounding bone is compressed. The tumor is a highly malignant lesion, but when the imaging manifestations are not typical, the diagnosis is extremely difficult (4). It is hoped that the introduction of this case can provide reference for the early detection of intracranial EMCS in medical imaging examination. The clinical, radiographic, and pathological findings are described with a review of the literature, which focused on the imaging characteristics facilitating diagnosis. We present the following case in accordance with the CARE reporting checklist (available at https://tcr.amegroups.com/article/view/10.21037/tcr-21-2547/rc).

Case presentation

A 20-year-old male patient was admitted to our hospital due to headache and dizziness for two months, without nausea, vomiting, limb convulsions and loss of consciousness during the illness. The clinical feature of this case is a young male patient with chronic onset and long course of disease. The patient came to the hospital because of dizziness and headache. The imaging results show that the tumor volume is large, but the clinical symptoms are mild. The tumor is located directly below the skull in the right parietal lobe and occipital region. His neurological examinations including hemiparesis and sensory disturbance were unremarkable. Meningeal irritation and pathological signs (such as the Oppenheim sign, Chaddock sign and Babinski sign) were negative. Laboratory tests suggested no significant abnormality. Pre-contrast computed tomography (CT) revealed a large slightly hyperdense mass with irregularly lobulated margins in the right parietal and occipital region (*Figure 1A*). The density of the lesion was uniform with an average of 54 Hounsfield unit (HU), and multiple patchy calcifications were observed in peripheral of the lesion. Post-contrast CT showed mild homogeneous enhancement, with an average density of approximately 79 HU (*Figure 1B*). On CT angiography (CTA) the lesion was supplied by the branch of the right middle cerebral artery, and the tumor vessels within the lesion were rich and tortuous. The inner table of right parietal bone adjacent to the mass was compressed, thickened, and eroded (*Figure 1C*). Magnetic resonance imaging (MRI) demonstrated a well-defined multi-lobulated mass based along the inner table of the right parietal bone for 8.7 cm × 6.6 cm × 7.5 cm in size. The lesion mainly exhibited intermediate and hypo-intensity on T1-weighted images (T_1WI) and slight hyper-intensity on T2-weighted images (T_2WI) (*Figure 2A,2B*). There was an extremely high intensity rim of cerebral spinal fluid (CSF) around the mass and low intensity flow-void vessel in lesion on T_2WI (*Figure 2B*). No intratumoral hemorrhage and peritumoral edema was observed. After intravenous administration of gadolinium-diethylene trianmine pentaacetic acid (Gd-DTPA), the mass demonstrated heterogeneous remarkable enhancement and "dural tail" sign was also noted (*Figure 2C,2D*). During the operation, it can be seen that the tumor erodes the skull and dura, and the tumor is closely adhered to the dura. Diffusion weighted imaging (DWI) showed nonhomogeneous hyperintensity and the lowest apparent diffusion coefficient (ADC) value was approximately 0.563×10^{-3} mm^2/s (*Figure 2E,2F*), the average value was approximately 0.572×10^{-3} mm^2/s. The lateral ventricle in the right side was compressed and narrowed, and the midline structure shifted about 1.4 cm to the left. Obstructive hydrocephalus was not found. The patient underwent resection of the right parietal and occipital mass after completing preoperative examination. The patients were treated with hemostasis, anti-infection, prevention of epilepsy and enhancement of resistance. Grossly, the tumor was grayish brown in color and hard with clear boundaries. On histopathological evaluation, the lesion was composed of malignant small cells and well-differentiated chondrocytes on hematoxylin-eosin (H&E) stain. The chondrocytes formed an island structure which was surrounded by diffuse distribution of small cells (*Figure 3A*). The small cells were obviously heteromorphic with round or oval shape and deeply stained nucleus (*Figure 3B*). The mitotic figures were easy to be found. Immunohistochemical examination results showed S-100 was positive for well-differentiated chondrocytes in the cartilaginous island, and negative for peripheral small cells (*Figure 3C*). The small cells showed partly positive for Vimentin (*Figure 3D*) and its membrane was diffuse CD99 positive (*Figure 3E*). Cytokeratin, Glial-fibrillary acidic protein (GFAP) (*Figure 3F*), epithelial membrane antigen (EMA) and CD34 were negative for all small cells and chondrocytes. CD99 were negative for chondrocytes. The pathological diagnosis was enhancement of resistance.

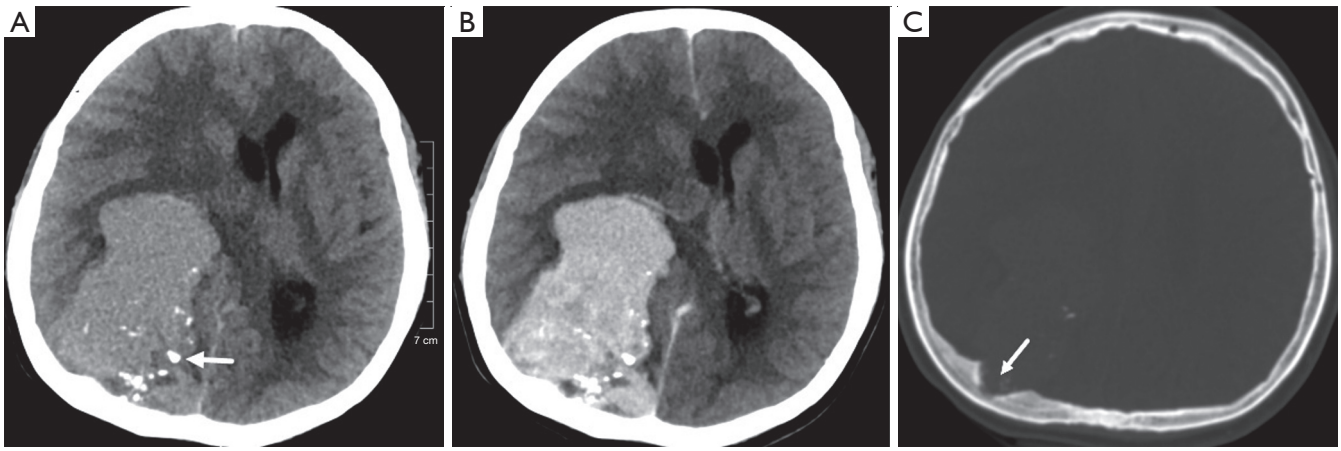

Figure 1 CT images. (A) Pre-contrast CT revealing a large slightly hyperdense mass (54 HU) with irregularly lobulated margins in the right parietal and occipital region and multiple patchy calcifications in peripheral of the lesion (arrow). (B) Post-contrast CT showing mild homogeneous enhancement (79 HU). (C) The inner table of right parietal bone adjacent to the mass was compressed, thickened, and eroded (arrow). CT, computed tomography; HU, Hounsfield unit.

Followed up postoperatively with serial MRI every three months, the patient was alive without obvious symptoms and evidence of recurrence for 9 months. Written informed consent was obtained from the patient for publication of this case report and accompanying images.

All procedures performed in this study were in accordance with the ethical standards of the institutional and/or national research committee(s) and with the Helsinki Declaration (as revised in 2013). Written informed consent was obtained from the patient for publication of this case report and accompanying images. A copy of the written consent is available for review by the editorial office of this journal.

Discussion

According to the WHO classification of bone tumors (fifth edition) (5), chondrosarcoma includes four histopathological subtypes, such as classic, mesenchymal, clear cell and dedifferentiated subtype, while there are only classic and mesenchymal subtypes to be found intracranially according to previous reports (1,6). The pathogenesis of intracranial EMCS remains unclear, with two hypotheses presented in literature. The popular theory is that the intracranial EMCS originates from the mesenchymal elements of the central nervous system, such as primitive multipotent interstitial cells or their mature descendants which have the potential to differentiate into chondrosarcoma (7). It is also believed that the intracranial EMCS possibly arises from the fibroblasts or partially differentiated chondroblast in the meninges (8). The present case supports the latter theory because the lesion is located beneath the skull and outside the cerebral convexity.

Intracranial EMCS is more common in young people aged from 10 to 30 years old with a slight female predominance, but the classic type has no obvious age and sexual propensity (9). Intracranial location is the most common site of EMCS (8). Previous reports showed that intracranial chondrosarcoma usually originated from the synchondroses of the skull base, particularly the sphenoid bone and the clivus ossis occipitalis (7,8). But Chen *et al.* (10) found that intracranial EMCS was more in the frontal parietal area than at the skull base. It was noteworthy that most of the intracranial chondrosarcoma near the superior sagittal sinus were mesenchymal subtype, and the other subtypes were rare here (7,11). The tumor in present case was located just beneath the skull in the right parietal and occipital regions, so that the leptomeningeal tissue might be a possible origin, and the age of the patient is also consistent with that in the literature report.

On imaging studies, traditional chondrosarcoma showed extremely high signal intensity on T_2WI and have a typical cartilage calcification and cellular enhancement, but intracranial EMCS had no such characteristics (12). Intracranial EMCS is a highly malignant disease, and the preoperative diagnosis is very difficult. However, CT

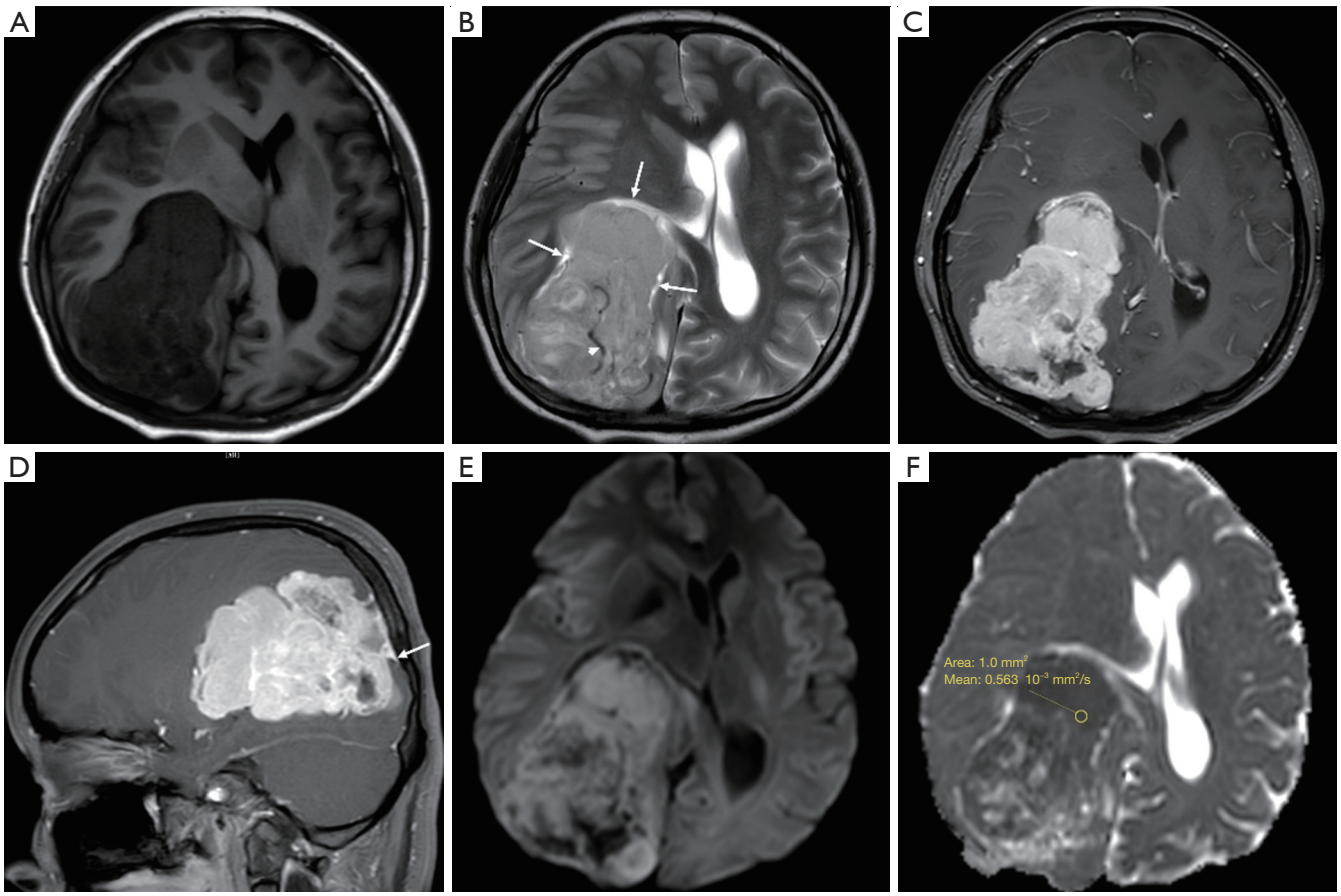

Figure 2 MRI images. (A,B) MRI demonstrating a well-defined multi-lobulated mass based along the inner table of the right parietal bone. The lesion exhibiting intermediate and hypo-intensity on T_1WI and slight hyper-intensity on T_2WI with extremely high intensity rim of CSF (arrows) around the mass and low intensity flow-void vessel (arrowhead). The lateral ventricle in the right side was compressed and narrowed, and the midline structure shifted to the left. (C,D) The mass demonstrated heterogeneous remarkable enhancement and "dural tail" sign was also noted (arrow). (E) DWI showed nonhomogeneous hyperintensity. (F) The lowest ADC value was approximately 0.563×10^{-3}mm^2/s. MRI, magnetic resonance imaging; CSF, cerebral spinal fluid; DWI, diffusion weighted imaging; ADC, apparent diffusion coefficient.

and MRI are very important for the clinical diagnosis and decision-making of intracranial EMCS. Imaging examination can accurately describe the disease, including the changes of size, density and signal, and the anatomical relationship around the tumor. These are very important for the diagnosis and differential diagnosis of the disease, especially the description of calcification, adjacent meninges and bone. It also can provide important information for the choice of surgical method. For highly malignant tumors, the clinical problem that needs to be paid attention to is postoperative recurrence, so CT and MRI are important monitoring methods. During routine reexamination, focus on the changes of operation area. CT usually revealed an isodense/hyperdense mass with irregular morphology and various degrees of calcification. The tumor was usually large in size, well-defined, and mostly lobulated in shape. MRI showed low signal intensity on T_1WI and slightly high signal intensity on T_2WI with modest to significant enhancement on CT and MRI after contrast agent administrated. Intracranial EMCS was an extracerebral tumor and closely related to the meningeal membrane, so "dural tail" sign could be commonly observed (12,13). The average value was approximately 0.572×10^{-3} mm^2/s, indicating limited diffusion. Mean ADC values

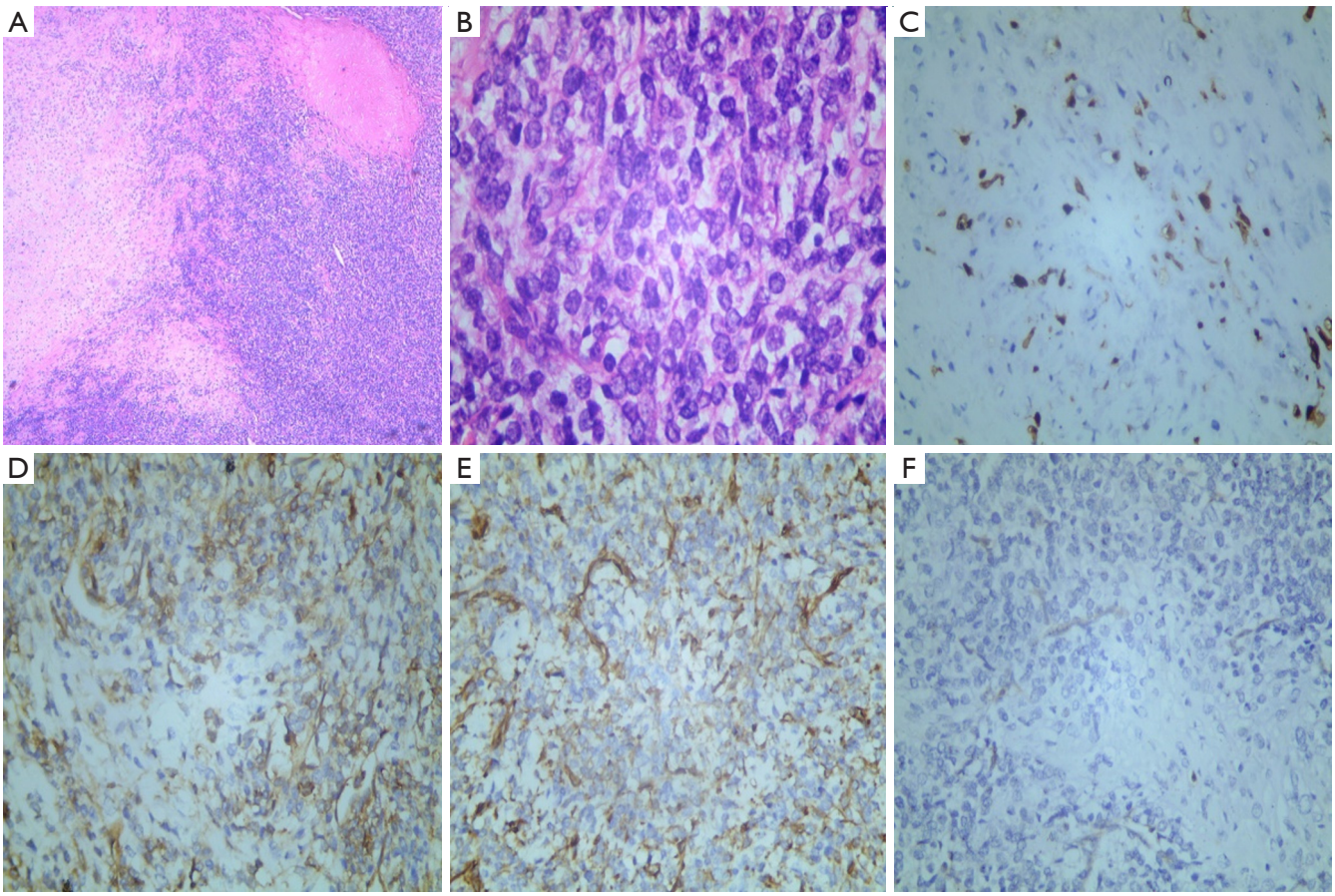

Figure 3 Histology of the lesion. H&E stained surgical resection of intracranial EMCS demonstrating well-differentiated chondrocytes forming an island structure (A, magnification ×40) surrounded by diffuse distribution of heteromorphic small cells with deeply stained nucleus and mitotic figures (B, magnification ×400). (C) S-200 was positive for well-differentiated chondrocytes in the cartilaginous island, and negative for peripheral small cells (magnification ×200). The small cells membrane was diffuse CD99 positive (D, magnification ×200), and its showing partly positive for vimentin (E, magnification ×200), negative for GFAP (F, magnification ×200). EMCS, extraskeletal mesenchymal chondrosarcoma; H&E, hematoxylin-eosin; GFAP, glial-fibrillary acid protein.

in meningiomas was reported to range from 0.80×10^{-3} to 0.96×10^{-3} mm^2/s (14). According to the research showed the mean ADC value of chondrosarcomas of the skull base; $2.05\pm0.26\times10^{-3}$ and $2.02\pm0.14\times10^{-3}$ mm^2/s, the ADC value of intracranial chondrosarcoma was more than 2.0×10^{-3} mm^2/s overall (15). The degree of differentiation of tumor can reflect the benign and malignant of tumor. The lower the degree of differentiation, the higher the degree of malignancy, the more obvious the cell abnormity, the increase of nucleocytoplasmic ratio and the close arrangement of cells, resulting in the limited diffusion of water molecules inside and outside the cells in the tissue, and the corresponding decrease of ADC value. Although the present case was large, there was no peritumoral edema, intratumoral hemorrhage or necrosis to be observed because of abundance of blood supply and slow growth. Due to slow-growing nature, there might be compression and erosion on the adjacent bone.

Although the imaging findings are characteristic, intracranial EMCS is still easy to be misdiagnosed and should be differentiated from the following intracranial tumors: (I) meningioma: both meningioma and intracranial EMCS have similar locations, blood-rich characteristics, and calcification and show iso-density/hyper-density on CT plain scan, but patients with meningioma are older than patients with intracranial EMCS (16). In addition,

they have different shape of calcification which are sand-like or flake for meningioma but spot and plaque for intracranial EMCS. Furthermore, the calcification range for EMCS is more extensive than that of meningioma. Bone adjacent to meningioma could have hyperplasia, whereas the skull adjacent to intracranial EMCS could be depressed and eroded, even destructed. (II) Hemangiopericytoma: both hemangiopericytoma and intracranial EMCS are significantly enhanced on post-contrast CT/MR imaging and have "dural tail" sign, but they have different predilection of site and age (17). Also, hemangiopericytoma do not contain chondrogenic composition, so the shape of calcification was different from intracranial EMCS. (III) Oligodendroglioma: oligodendroglioma and intracranial EMCS have different predilection site, enhancement degree and calcifications. Oligodendroglioma tends to occur in the brain parenchyma away from skull or meninges. Calcification is mostly curved strip, and the enhancement degree on post-contrast imaging is lighter than that of the intracranial EMCS (18).

When the imaging of intracranial EMCS is atypical and the identification is difficult, the final diagnosis depends on pathological examination. On histopathology, intracranial EMCS was characterized by bidirectional differentiation of undifferentiated small cells and hyaline cartilaginous island with different degrees of differentiation (1,5,19). Small undifferentiated mesenchymal cells were round or short spindle with deeply stained nucleus and mitotic figures. The size of hyaline cartilaginous island scattering in the small mesenchymal cells was different and the distribution was inhomogeneous (5). Some chondrocytes were well-differentiated with cartilage lacunae, and the other chondrocytes were poorly differentiated which were like the undifferentiated small cells (1,8). Immunohistochemically, S-100 was positive for well-differentiated chondrocytes, and negative for peripheral small cells. The small cells showed partly positive for Vimentin and its membrane was diffuse CD99 positive. Whereas CK, GFAP, EMA and CD34 were negative for all small cells and chondrocytes (8,19,20). These features can easily differentiate chondrosarcoma from meningioma, hemangiopericytoma, and oligodendroglioma.

Conclusions

In conclusion, we described a rare case of intracranial EMCS focusing on the CT and MRI features. Imaging findings include large, well-defined, hyperdense mass with lobulated morphology and various degrees of calcifications, often accompanied by modest to significant enhancement on CT and MRI after contrast agent administrated and bone compression and erosion, without necrosis or cystic changes. The difficulty of CT and MRI diagnosis of intracranial EMCS lies in that the location of tumor onset is not characteristic, and the density and signal are like most intracranial tumors. Because it is a highly malignant tumor, a combination of clinic, pathology, and imaging is necessary to avoid misdiagnosis. It is hoped that the introduction of this case can provide reference for the early detection of intracranial EMCS in medical imaging examination.

Acknowledgments

Funding: None.

Footnote

Reporting Checklist: The authors have completed the CARE reporting checklist. Available at https://tcr.amegroups.com/article/view/10.21037/tcr-21-2547/rc

Peer Review File: Available at https://tcr.amegroups.com/article/view/10.21037/tcr-21-2547/prf

Conflicts of Interest: All authors have completed the ICMJE uniform disclosure form (available at https://tcr.amegroups.com/article/view/10.21037/tcr-21-2547/coif). The authors have no conflicts of interest to declare.

Ethical Statement: The authors are accountable for all aspects of the work in ensuring that questions related to the accuracy or integrity of any part of the work are appropriately investigated and resolved. All procedures performed in this study were in accordance with the ethical standards of the institutional and/or national research committee(s) and with the Helsinki Declaration (as revised in 2013). Written informed consent was obtained from the patient for publication of this case report and accompanying images. A copy of the written consent is available for review by the editorial office of this journal.

References

1. Bloch OG, Jian BJ, Yang I, et al. A systematic review of intracranial chondrosarcoma and survival. J Clin Neurosci 2009;16:1547-51.
2. Shabani S, Kaushal M, Kaufman B, et al. Intracranial Extraskeletal Mesenchymal Chondrosarcoma: Case Report and Review of the Literature of Reported Cases in Adults and Children. World Neurosurg 2019;129:302-10.
3. Chhabra R, Tripathi M, Patra DP, et al. Primary Intracranial Extraskeletal Mesenchymal Chondrosarcoma: Clinical Mimicry as Glomus Jugulare. Ann Neurosci 2017;24:181-6.
4. Xiao A, Li Z, He X, et al. A rare tentorial mesenchymal chondrosarcoma in posterior cranial fossa: case report. Neurol Neurochir Pol 2014;48:287-91.
5. Choi JH, Ro JY. The 2020 WHO Classification of Tumors of Bone: An Updated Review. Adv Anat Pathol 2021;28:119-38.
6. Korten AG, ter Berg HJ, Spincemaille GH, et al. Intracranial chondrosarcoma: review of the literature and report of 15 cases. J Neurol Neurosurg Psychiatry 1998;65:88-92.
7. Oruckaptan HH, Berker M, Soylemezoglu F, et al. Parafalcine chondrosarcoma: an unusual localization for a classical variant. Case report and review of the literature. Surg Neurol 2001;55:174-9.
8. Aigner T, Loos S, Müller S, et al. Cell differentiation and matrix gene expression in mesenchymal chondrosarcomas. Am J Pathol 2000;156:1327-35.
9. Beena D, Kattoor J, Mathews A, et al. Mesenchymal Chondrosarcoma-A Retrospective study. Gulf J Oncolog 2021;1:54-8.
10. Chen JY, Hsu SS, Ho JT. Extraskeletal intracranial mesenchymal chondrosarcoma: case report and literature review. Kaohsiung J Med Sci 2004;20:240-6.
11. Kathiravel Y, Finnis ND. Primary falcine chondrosarcoma. J Clin Neurosci 2008;15:1406-9.
12. Sadashiva N, Sharma A, Shukla D, et al. Intracranial Extraskeletal Mesenchymal Chondrosarcoma. World Neurosurg 2016;95:618.e1-6.
13. Chi J, Zhang M, Kang J. Classical intracranial chondrosarcoma: A case report. Oncol Lett 2016;12:4051-3.
14. Surov A, Gottschling S, Mawrin C, et al. Diffusion-Weighted Imaging in Meningioma: Prediction of Tumor Grade and Association with Histopathological Parameters. Transl Oncol 2015;8:517-23.
15. Kojima D, Beppu T, Saura H, et al. Apparent diffusion coefficient and arterial spin labeling perfusion of conventional chondrosarcoma in the parafalcine region: a case report. Radiol Case Rep 2017;13:220-4.
16. Saloner D, Uzelac A, Hetts S, et al. Modern meningioma imaging techniques. J Neurooncol 2010;99:333-40.
17. Chen Q, Chen XZ, Wang JM, et al. Intracranial meningeal hemangiopericytomas in children and adolescents: CT and MR imaging findings. AJNR Am J Neuroradiol 2012;33:195-9.
18. Smits M. Imaging of oligodendroglioma. Br J Radiol 2016;89:20150857.
19. Shakked RJ, Geller DS, Gorlick R, et al. Mesenchymal chondrosarcoma: clinicopathologic study of 20 cases. Arch Pathol Lab Med 2012;136:61-75.
20. Ma X, Meng G, Wang K, et al. The Differences Between Intracranial Mesenchymal Chondrosarcoma and Conventional Chondrosarcoma in Clinical Features and Outcomes. World Neurosurg 2019;122:e1078-82.

Cite this article as: Chu J, Ma H, Wang Y, Li K, Liao C, Ding Y. CT and MRI findings of intracranial extraskeletal mesenchymal chondrosarcoma—a case report and literature review. Transl Cancer Res 2022;11(9):3409-3415. doi: 10.21037/tcr-21-2547

